Supporting Information

Controllable growth of wafer-scale PdS and PdS_2 nanofilms via chemical vapor deposition combined with electron beam evaporation technique

Hui Gao[1#], Hongyi Zhou[1#], Yulong Hao[2#], Guoliang Zhou[3], Huan Zhou[1], Fenglin Gao[1], Jinbiao Xiao[1], Pinghua Tang[1] and Guolin Hao[1, 4*]

1. School of Physics and Optoelectronics and Hunan Institute of Advanced Sensing and Information Technology, Xiangtan University, Hunan 411105, P. R. China

2. College of Physics and Technology & Guangxi Key Laboratory of Nuclear Physics and Technology, Guangxi Normal University, Guilin 541004, P. R. China

3. Department of Electronic and Electrical Engineering, University of Sheffield, Sheffield S10 2TN, U. K

4. National Laboratory of Solid State Microstructures, Nanjing University, 210093, P. R. China

#These authors contribute equally to this work.

*Corresponding author. Tel.: +86 0731-58293749; fax: +86 0731-58298612.

E-mail: guolinhao@xtu.edu.cn

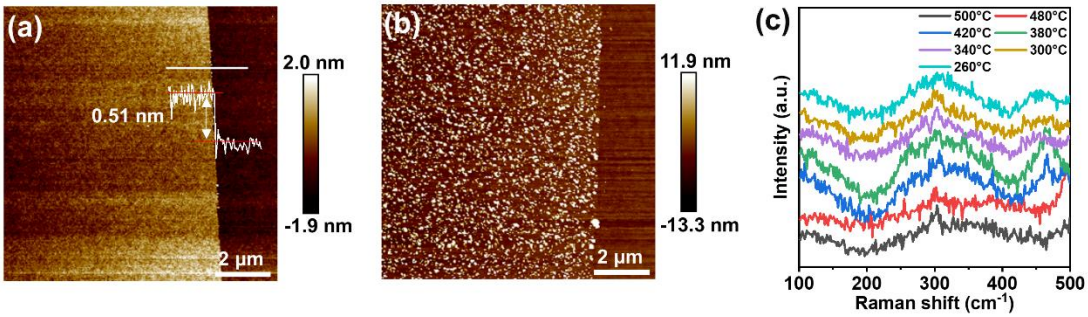

Fig. S1 (a) AFM image of the Pd film with pre-deposited thickness ~0.5 nm before and after sulfurization. (c) Raman spectra of as-prepared NFs under different sulfurization temperature.

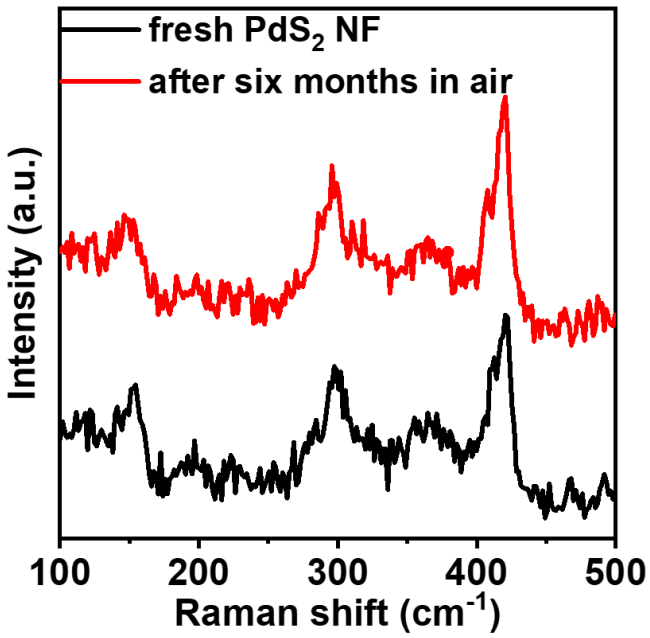

Fig. S2 Raman spectra of the fresh PdS_2 NF and after stored in air for six months.

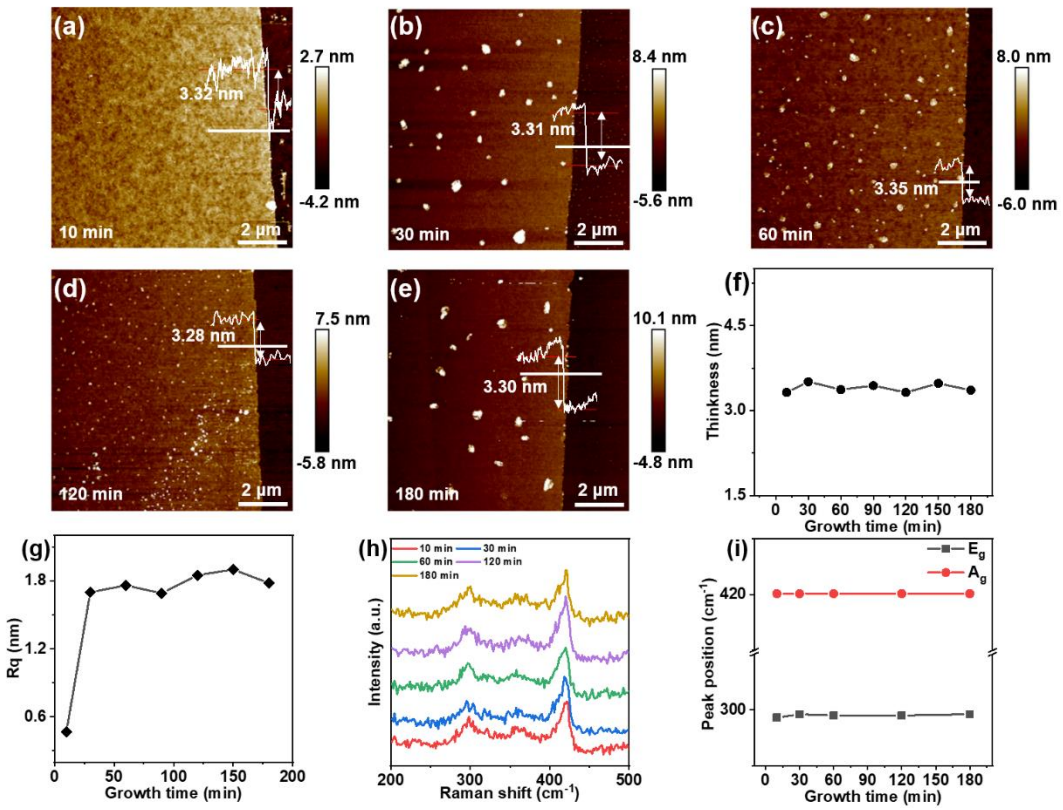

Fig. S3 (a-e) AFM images of the as-prepared PdS_2 NFs with different sulfurization time. (f, g) Thickness and Rq of the as-prepared PdS_2 NFs as a function of sulfurization time. (h) Raman spectra of as-prepared PdS_2 NFs with different sulfurization time. (i) Position of the A_g and E_g peaks as a function of sulfurization time.

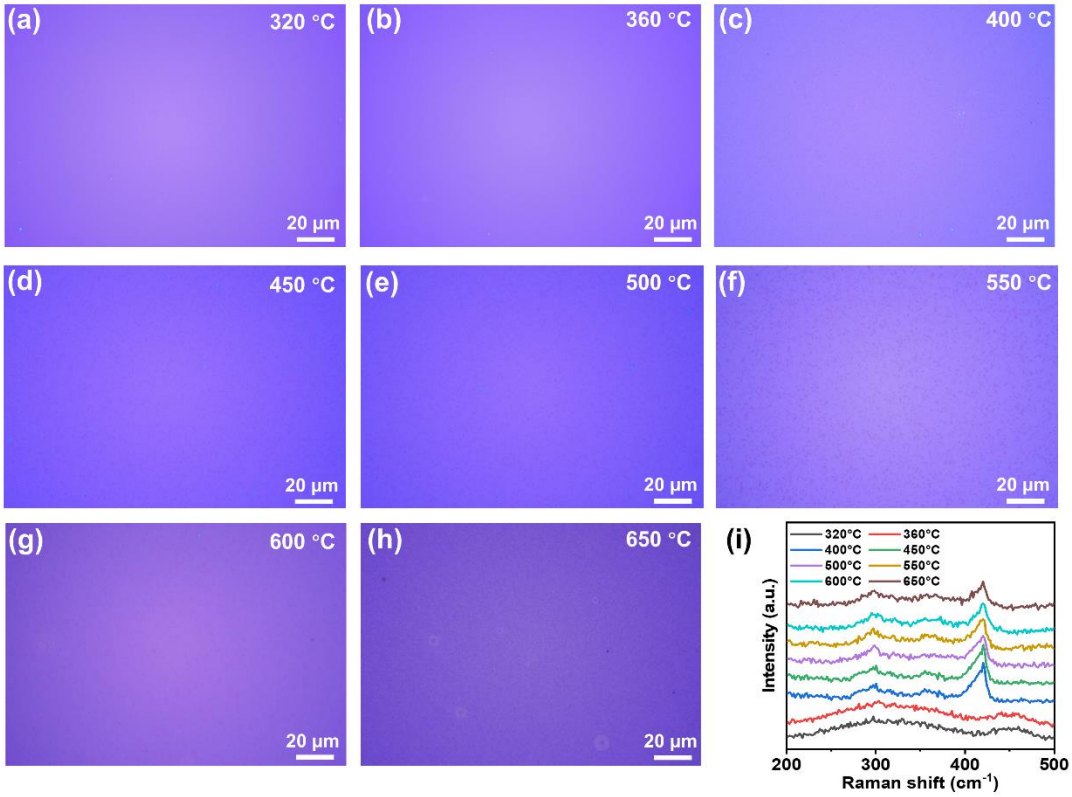

Fig. S4 (a-h) OM images of the as-prepared PdS_2 NF with different sulfurization temperature. (i) Raman spectra of as-prepared NFs under different sulfurization temperature.

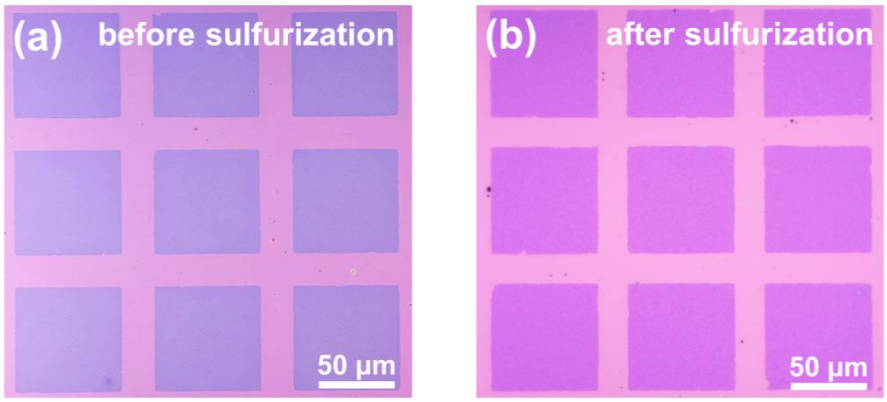

Fig. S5 (a) OM image of the 1 nm Pd pattern using the Cu grid as mask. (b) Corresponding OM image of the 1 nm Pd after sulfurization.

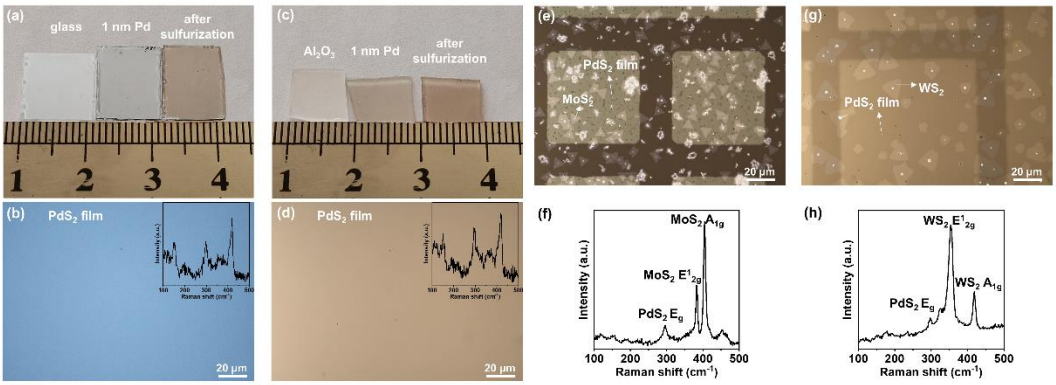

Fig. S6 (a, c) Photo images of as-prepared PdS_2 NFs grown on glass and Al_2O_3 substrates. (b, d) OM images of as-synthesized PdS_2 NFs. Inset: corresponding Raman spectra. (e) and (f) OM image and Raman spectrum of synthesized PdS_2-MoS_2 heterojunction. (g) and (h) OM image and Raman spectrum of synthesized PdS_2-WS_2 heterojunction.

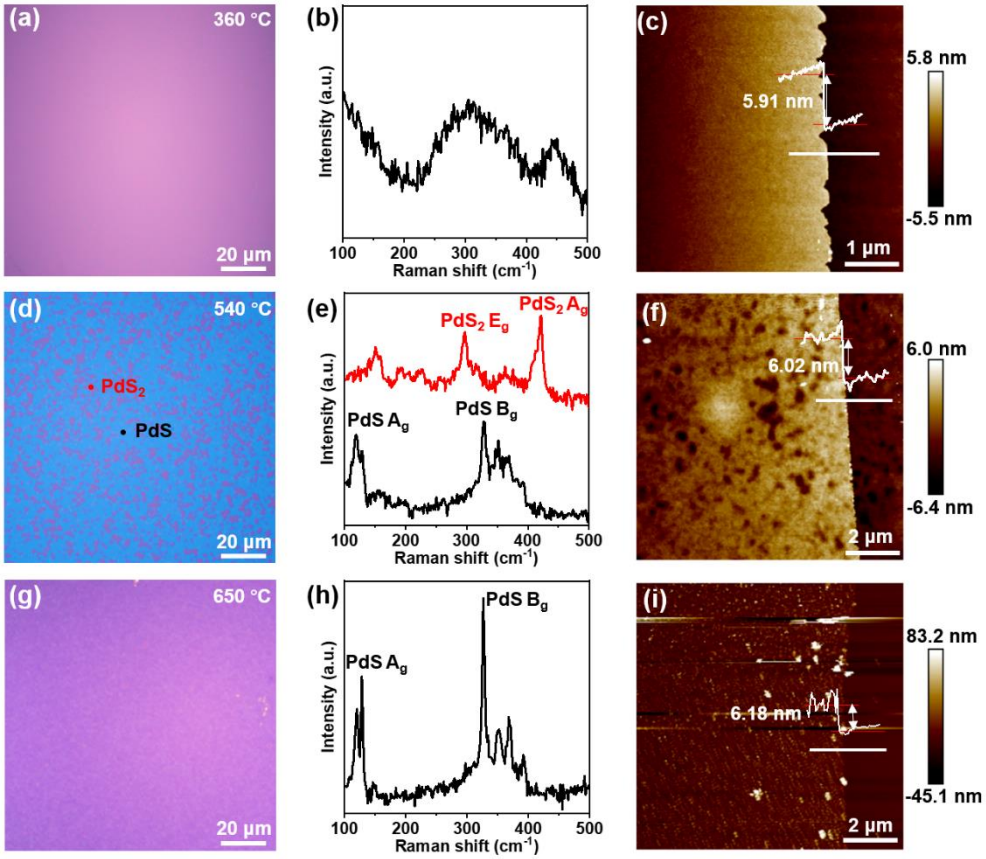

Fig. S7. (a, d, g) OM images of as-synthesized samples with different sulfurization

temperature: 360 °C, 540 °C, and 650 °C, respectively. (b, e, h) Corresponding Raman spectra of the synthesized NFs. (c, f, i) Corresponding AFM images of as-prepared products.

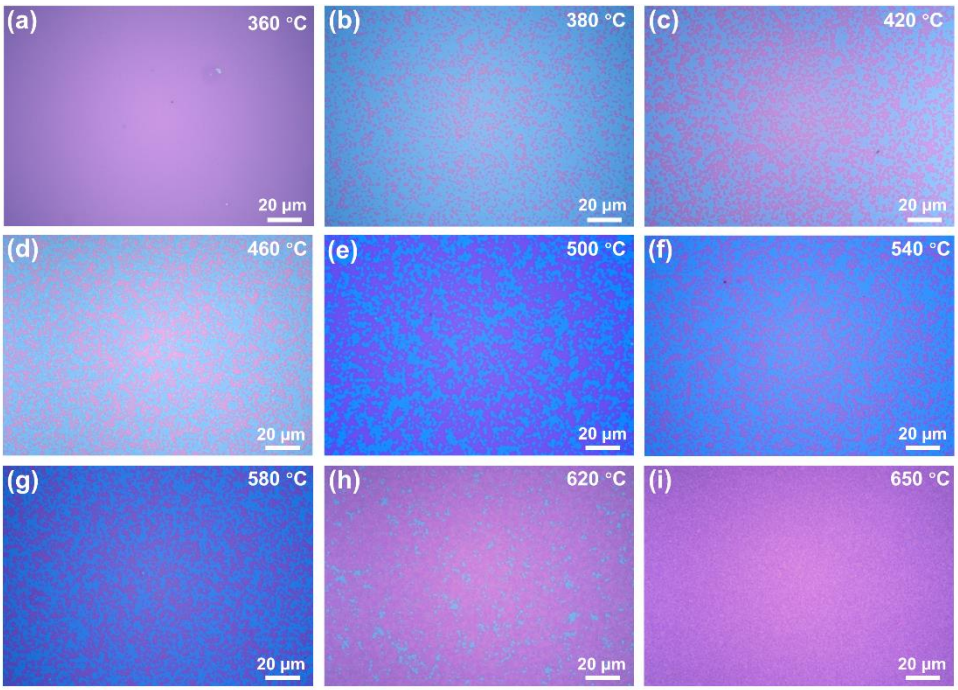

Fig. S8 (a-i) OM images of the as-prepared samples with different sulfurization temperature. The thickness of pre-deposited Pd is 2 nm.

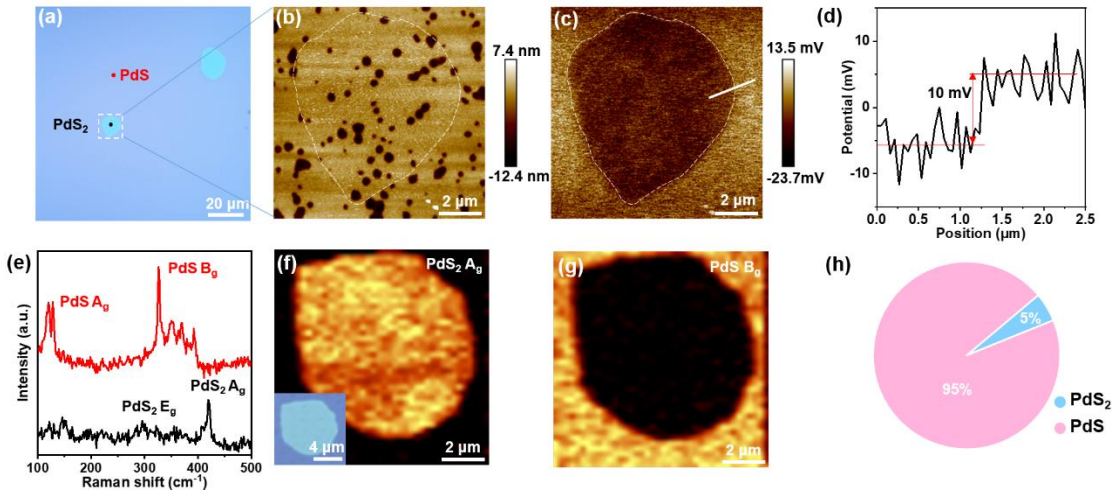

Fig. S9 (a) OM image of hybrid PdS-PdS_2 NF (the thickness of pre-deposited Pd ~ 4 nm). (b) Corresponding AFM image of as-synthesized PdS-PdS_2 hybrid NF obtained

as marked in (a). (c) Corresponding surface potential image (d) The surface potential profile alone the white line. (e) Raman spectra taken from the red and black points marked in (a). (f) Raman intensity mapping (A_g mode) of PdS_2 NF. Inset: corresponding OM image. (g) Raman intensity mapping (B_g mode) of PdS NF. (h) Statistical diagram of area ratio of PdS_2 and PdS for the obtained hybrid NF.

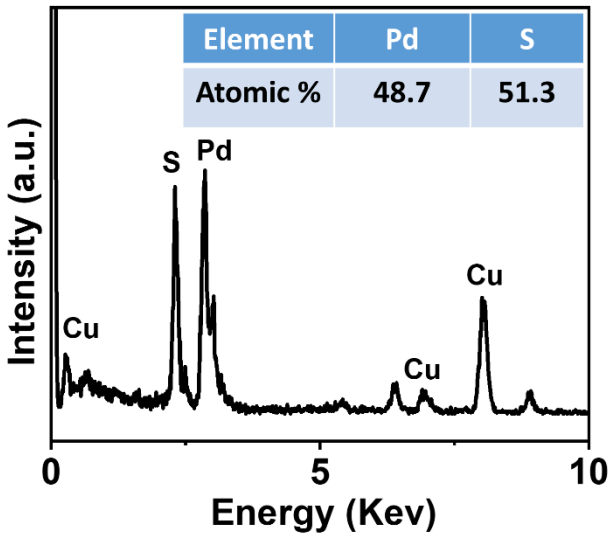

Fig. S10 EDS analysis of the PdS NF.

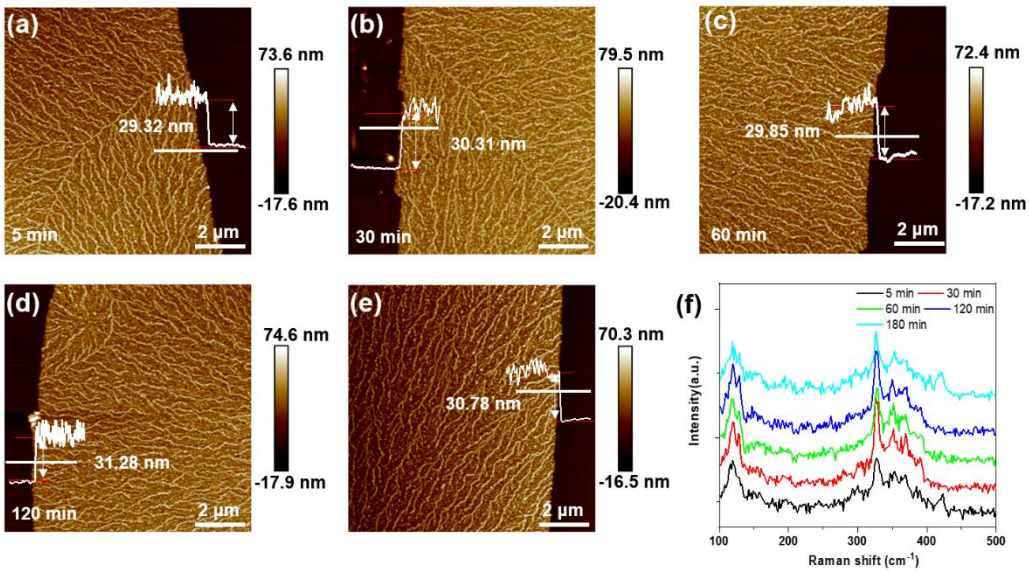

Fig. S11 (a-e) AFM images of the as-prepared PdS NFs with different sulfurization time. (f) Corresponding Raman spectra.

The calculation of the detailed Gibbs free energy is given as follows：

$$\Delta_r H_m^0(T_1)=\Sigma\nu_B\Delta_f H^0(\text{product})-\Sigma\nu_B\Delta_f H^0(\text{reactant}) \quad (1)$$

$$\Delta_r H_m^0(T_1)=\Sigma\gamma_B\Delta_f H^0(\text{product})-\Sigma\gamma_B\Delta_f H^0(\text{reactant}) \quad (2)$$

$$\Delta_r S_m^0(T_1)=\Sigma\gamma_B S^0(\text{product})-\Sigma\gamma_B S^0(\text{reactant}) \quad (3)$$

$$\Delta C_p=\Sigma\gamma_B C_p(\text{product})-\Sigma\gamma_B C_p(\text{reactant}) \quad (4)$$

$$\Delta_r H_m^0(T_2)=\Delta_r H_m^0(T_1)+\Delta C_p(T_2-T_1) \quad (5)$$

$$\Delta_r S_m^0(T_2)=\Delta_r S_m^0(T_1)+\Delta C_p \text{In}\left(\frac{(T_2}{(T_1}\right) \quad (6)$$

$$\Delta G_m^0=\Delta_r H_m^0(T_2)-T\Delta_r S_m^0(T_2) \quad (7)$$

Where $\Delta rH^0{}_m(T_1)$ and $\Delta rS^0{}_m(T_1)$ represent the standard enthalpy and the standard entropy of reaction at 298 K. T_2 is the reaction temperature (K). The relative thermodynamic data of the reactants and products in the reaction are shown in Table S1.

Table S1: Enthalpies and Gibbs energies of formation, entropie, and heat capacities of the elements and inorganic compounds, see at https://janaf.nist.gov/ (NIST Standard Reference Database 13)

substance	**Phase**	**$H°_{298k}$ (J/mol)**	**C_p**	**$S°_{298k}$ (J/mol)**
Pd	Solid	0	25.981	37.823
S_2	Gas	128658	32.443	228.028
PdS	Solid	-70710	43.399	56.484
PdS_2	Solid	-78241	65.879	87.864

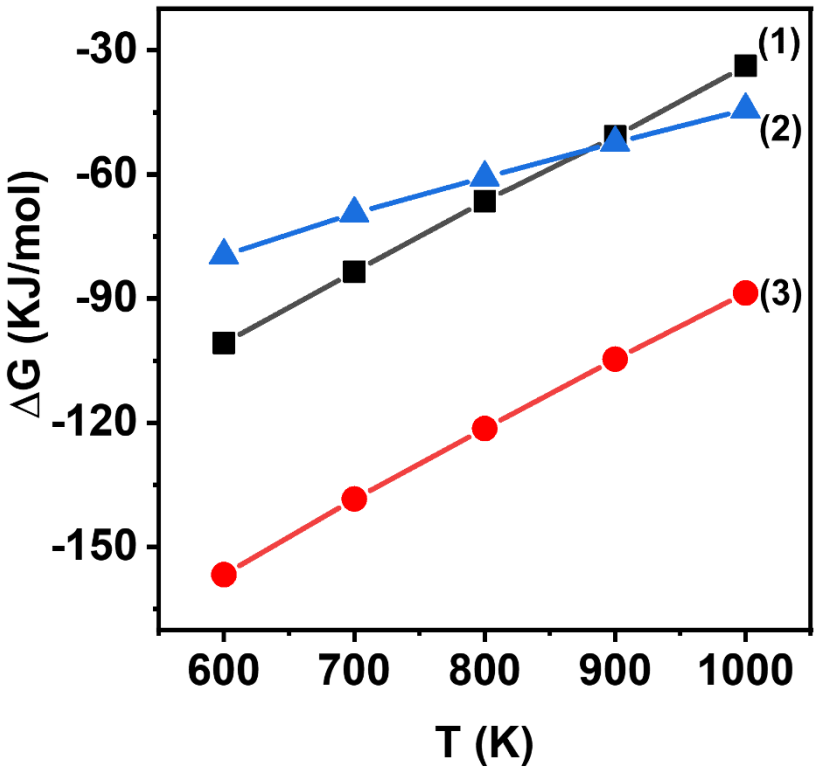

Fig. S12. (a) Calculations of Gibbs energy for the reactions described in equations 1-3 (expressed per mole of Pd).

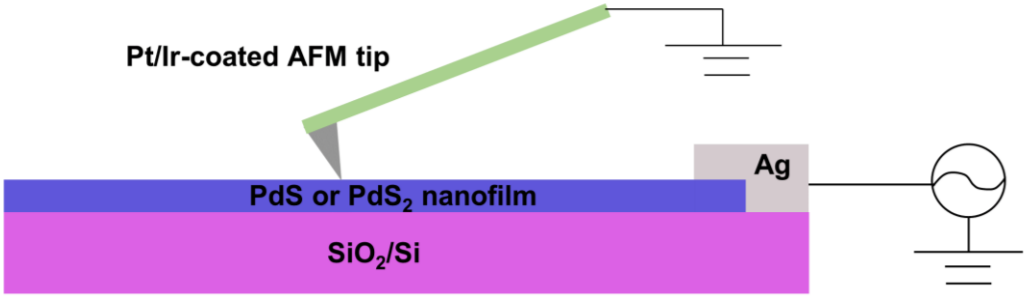

Fig. S13. Schematic diagram of the C-AFM electrical measurement.

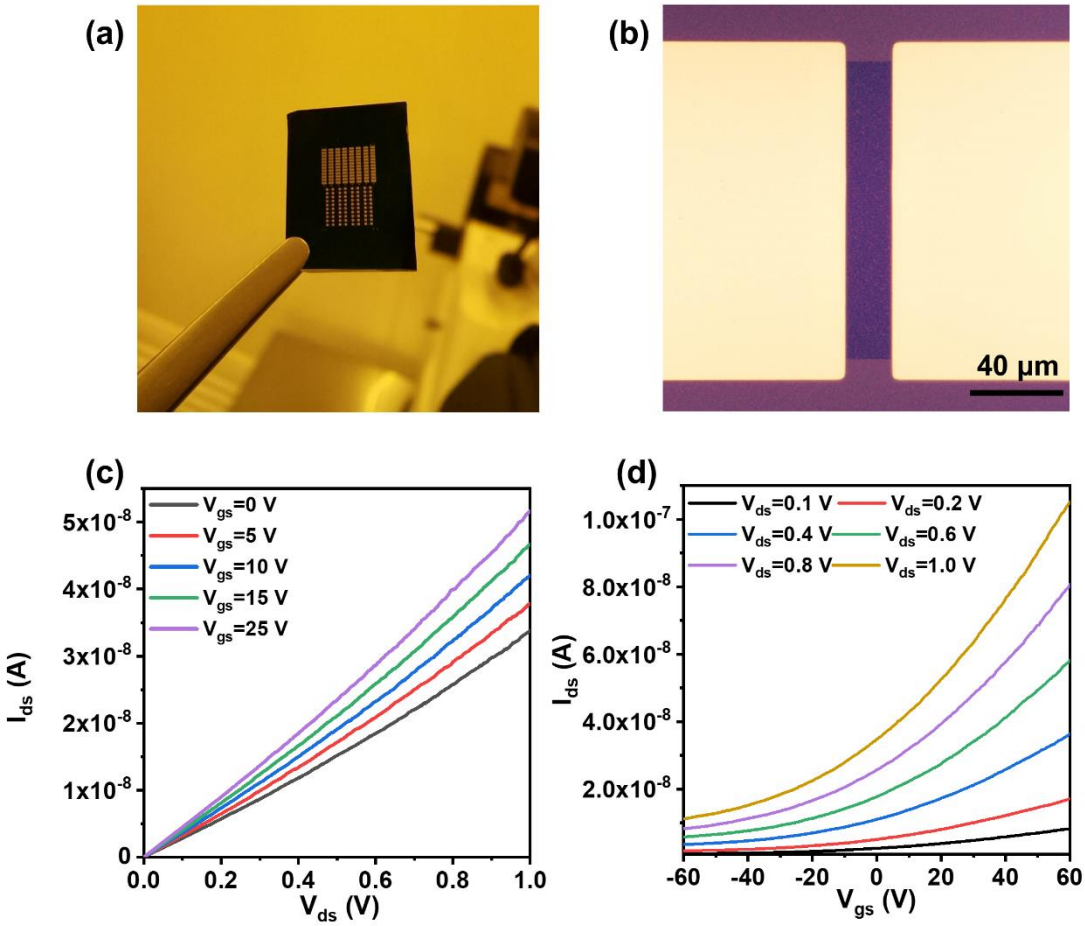

Fig. S14. (a) Photo image of as-prepared PdS_2 TFT. (b) OM image of the PdS_2 device. (c) Output characteristics of the PdS_2 TFT. (d) Transfer characteristics of PdS_2 TFT.